RESEARCH ON LIME ROTARY KILN TEMPERATURE PREDICTION BY MULTI-MODEL FUSION NEURAL NETWORK BASED ON DYNAMIC TIME DELAY ANALYSIS

Zhimin Liu[1,3,4*], Pengzhou Meng[1], Yincheng Liang[2], Jiahao Li[1], Shiyu Miao[1], Yue Pan[1,3,4]

[*1]Mechanical and Electrical Engineering Institute, Hebei University of Engineering, Handan, 056038, China;

[2]Shandong Water Conservancy Vocational College, Department of information engineering, Rizhao, 276826, China;

[3]Key Laboratory of Intelligent Industrial Equipment Technology of Hebei Province(Hebei University of Engineering),Handan, 056038, China

[4] Collaborative Innovation Center for Modern Equipment Manufacturing of Jinan New Area, Hebei Province, Handan, 056038, China

* Corresponding author; E-mail: lzm15212@126.com

The lime rotary kiln systems are widely used in the metallurgical industry, where the combustion state is exceptionally complex, and it is difficult to predict and control the calcined zone's temperature. The lime rotary kiln system uses the entropy and grey correlation model, combining the lime rotary kiln operation process to determine the input and output characteristics of the model. Then, it analyzes the time lag and inertia in the lime rotary kiln combustion system to compensate for the temperature prediction in the lime rotary kiln by using the CNN-BILSTM-OC model. Correcting the expected output results with the actual situation. The experimental analysis shows that the proposed model has a higher prediction accuracy than others. The maximum relative error calculated for the future temperature prediction is 0.2098%, while the generalized average of the root mean square error of the model under different working conditions is 0.9639. The generalized average of the mean absolute error is 0.6683, which shows that the model has a strong generalization ability to meet practical applications.

Key words*: lime rotary kiln system; the compensation of the time lag of the dynamic error; entropy and grey correlation model; temperature prediction*

1. Introduction

The lime rotary kiln system is widely used in mining, iron and steel smelting, and other industries; its calcined belt temperature changes the quality of finished products, and material heat exchange has a more significant impact. A lime rotary kiln in a combustion state is a considerable time lag, multi-coupling, nonlinear complex system, so it is more difficult to control the temperature of the lime rotary kiln in the combustion state. Some intelligent lime rotary kiln models combined with deep learning have been widely used. Hu *et al*. [1] established a lime rotary kiln condition recognition

model based on migration learning and attention mechanism, realized feature migration and parameter sharing, and improved the model generalization ability. Urbano *et al.* [2] conducted mathematical modeling and numerical simulation of a lime rotary kiln to predict the kiln temperature and suggest control parameters through the model. Li *et al.* [3] proposed a DTDR-ALSTM dynamic time delay model, which can extract the features based on the dynamic relationship between the variables and establish a more accurate mathematical model. Tian *et al.* [4] proposed a predictive control model for lime rotary kiln temperature combining SVM and improved PSO. Zhang *et al.* [5] proposed a method for recognizing lime rotary kilns with different combustion states based on Otsu-Kmeans flame image segmentation and SVM using visual detection technology as a basis. Chen *et al.* [6] proposed utilizing several luminescent features and dynamic features of flame images to overcome the rapid temperature changes to predict the temperature condition inside a lime rotary kiln. Hu *et al.* [7] proposed a method for predicting the temperature of a lime rotary kiln based on a GRP-lstmGAN model by converting one-dimensional time-series data into two-dimensional image data and utilizing the feature-capturing ability of the time series. Xu *et al.* [8] proposed a structure containing a residual network and a two-way gated recurrent network to accurately predict the preheater outlet temperature utilizing an adaptive sliding window. Zheng *et al.* [9] used recurrent neural networks to establish a lime rotary kiln model by combining the mechanism of the lime rotary kiln combustion process to improve the accuracy of mathematical modeling. Wang *et al.* [10] proposed a weighted correlation vector machine model based on dynamic time delay estimation. Furthermore, they compensated the model's prediction accuracy based on the time delay difference. Okoji *et al.* [11] used the model for simulation and combined with BANN neural network to accurately predict the energy efficiency of a cement kiln. Li *et al.* [12] through optimization of the rotary kiln combustion process by the law of conservation of mass and energy. Although many scholars have made significant progress in related aspects, due to the complexity of the lime rotary kiln combustion model itself, many problems still lead to poor temperature prediction in the lime rotary kiln. This paper proposes a fusion neural network (CNN-BILSTM-OC) lime rotary kiln temperature prediction model based on dynamic error time lag compensation. First, we use the entropy weight method - gray correlation model to combine with the lime rotary kiln process to determine the input and output engineering of the model. Then, we use the error performance criterion method to determine the time lag and inertial order in the lime rotary kiln combustion system. Finally, we predict the temperature of the lime rotary kiln by a fuse CNN-BILSTM model and calculate the dynamic error compensation to obtain the final output results. This model's validity in this paper is verified by experimental simulation analysis.

2. Brief description of the rotary kiln system flows

Lime rotary kiln system mainly includes feeding, firing, finished product, and exhaust gas systems. Lime raw materials through the feeding belt and conveyor hopper are transported into the preheater for material heat reaction to complete the feeding action. Preheating is completed after the raw materials are added to the lime rotary kiln through the primary wind, secondary wind, and other combustion wind in the furnace body for high-temperature reaction. Finally, the finished product is fired through a vibrating screen and other equipment for classification, and the chain conveyor and belt storage to the receiving bin. The direction of gas flow is the opposite direction. The primary wind and secondary wind in the lime rotary kiln participate at the end of the combustion through the

downstream port back to the preheater. Then, reverse flow into the raw material silo dust system to participate in the dust. The lime rotary kiln's actual picture and process flow are shown in Fig. 1.

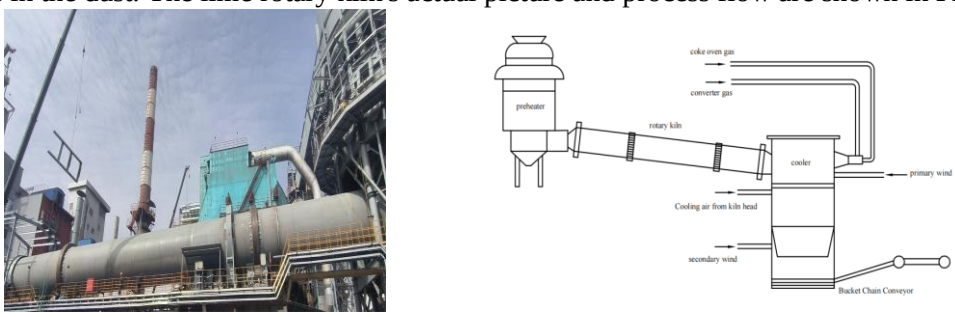

Fig. 1. Lime rotary kiln combustion systems

The most critical link in the entire calcination system is the lime rotary kiln firing system; for the benefit of the combustion state of the lime rotary kiln's internal temperature prediction and control for the lime rotary kiln for the analysis, sorted out the factors affecting the temperature of the lime rotary kiln contain coke oven gas flow, mixed gas flow, the primary air flow, the secondary air flow, the primary air pressure, the secondary air pressure, the central induced air pressure, kiln spindle frequency, the total amount of material fed and so on.

3. The lime rotary kiln data source analysis

3.1. Entropy and grey correlation mixed model analysis

The entropy weight method can transform some uncertainties in the system into definite outputs that can be precisely expressed. Entropy is mainly used to describe the degree of chaos in a system, and the smaller the value calculated by the entropy weighting method, the lower the degree of chaos and variability, and the factor occupies a relatively large weight in the system[13]. The initial data will be standardized according to Eq. (1). Then the standardized data will be solved for the information entropy according to Eq. (2), which can be calculated by substituting Eq. (3) to calculate the size of the weight coefficients of the influencing factors in the system.

$$\mathrm{r}_{ij} = \frac{x_{ij} - \min\left(x_i\right)}{\max\left(x_i\right) - \min\left(x_i\right)} \tag{1}$$

$$E_{\mathrm{j}} = -\ln\left(n\right)^{-1} \sum_{i=1}^{n} p_{ij} \ln p_{ij} \tag{2}$$

$$W_i = \frac{1 - E_i}{k - \sum E_i}\left(i = 1, 2, ..., k\right) \tag{3}$$

Where r_{ij} is the standardized data; i is the number of data items; j is the number of influencing factors items; E_j is the value of information entropy; n is the number; p_{ij} is the proportion of the i-th element in the j-th column; W_j is the entropy weight coefficient.

Where p_{ij} is computed as shown in Eq. (4), if $p_{ij} = 0$, then define $\lim_{p_{ij} \to 0} p_{ij} \ln p_{ij} = 0$.

$$p_{ij} = \frac{Y_{ij}}{\sum_{i=1}^{n} Y_{ij}} \tag{4}$$

The grey relational analysis model can analyze the similarities and differences between the trends of other independent variable factors and the movements of the target control group. After

selecting the target control group, non-significant factors are removed from the system based on the degree of correlation of all independent variable factors in the fuzzy system. Furthermore, calculating the gray correlation coefficient allows us to sort out the independent variables related to the output factors without specific manifestation. Factors with gray correlation coefficients below 0.5 are considered non-significant[14]. The gray correlation model $\zeta_i(k)$ is calculated as shown in Eq. (5):

$$\zeta_i(k) = \frac{\min_i \min_k \left|x_0(k) - x_i(k)\right| + \rho \max_i \max_k \left|x_0(k) - x_i(k)\right|}{\left|x_0(k) - x_i(k)\right| + \rho \max_i \max_k \left|x_0(k) - x_i(k)\right|} \tag{5}$$

Where $x_o(k)$ is the target control group; $x_i(k)$ is the current comparison group; ρ is the coefficient of discrimination.

The result of the entropy and grey correlation model visualization obtained is shown in Fig. 2.

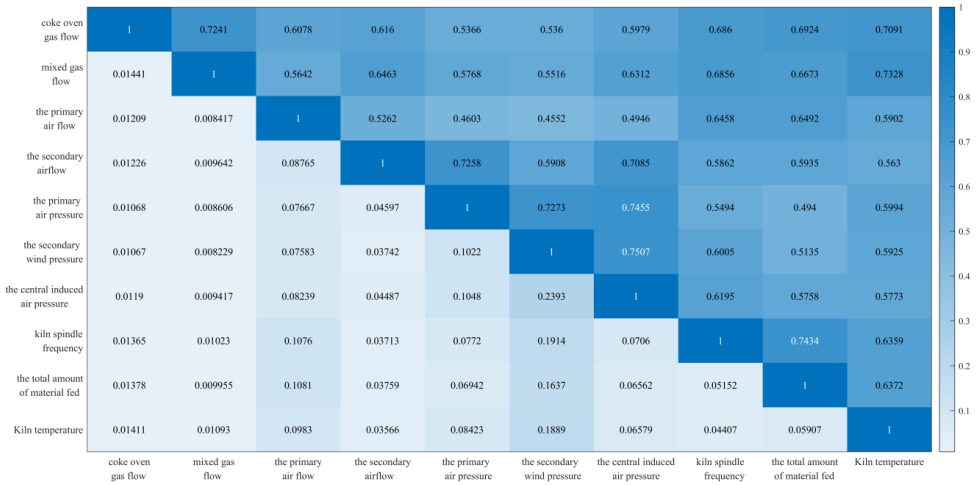

Fig. 2. Entropy and grey correlation degree hybrid model visualisation results

The identified factors were processed for correlation pre-analysis in Fig.2.Correlation pre-analysis of the above-identified control factors, where the upper right data are grey correlation coefficients, which are calculated by Equation (5), and the lower left data are entropy and grey correlation hybrid coefficients, which are derived by multiplying the weighting coefficients of the different influencing factors in the above Equation (3) by the grey correlation coefficients in Equation (5). Analysis of the lime rotary kiln system shows that the grey correlation coefficients for the different input factors are all greater than 0.5, and no non-significant factors need to be eliminated. Furthermore, the secondary air is analyzed as the main action factor affecting the combustion system of the lime rotary kiln, and its corresponding entropy and grey correlation degree mixing coefficient is 0.1889, much larger than the other influencing factors.

3.2. Data source preprocessing

The data collected in the field, may lead to the existence of recording errors in the initial data; we propose to use the Pauta criterion to deal with the gross errors. Through Eq. (6) and Eq. (7) eliminate errors in the initial dataset, and then Newton interpolation method as shown in Eq. (8) and Eq. (9), is used for the missing values and the blank values after the elimination of the gross errors to be filled to make the dataset more complete and smooth.

$$\sigma = \sqrt{\frac{\sum_{i=1}^{n}\left(x_i - x_p\right)^2}{n-1}} \tag{6}$$

$$\left|x_i - x\right| > 3\sigma \tag{7}$$

$$N_3(x) = f(x_0) + f[x_0, x_1](x - x_0) + f[x_0, x_1, x_2](x - x_0)(x - x_1) + \ldots$$
$$f[x_0, x_1, x_2, x_3](x - x_0)(x - x_1)(x - x_2) \tag{8}$$

$$f[x_0, x_1, \ldots, x_k] = \frac{f[x_0, x_1, \ldots, x_{k-2}, x_k] - f[x_0, x_1, \ldots, x_{k-1}]}{x_k - x_{k-1}} \tag{9}$$

where σ is the standard deviation; x_p is the mean; $N_3(x)$ is the Newton interpolated quotient; $f[x_0,x_1,\ldots,x_k]$ is the k-th difference quotient of $f(x)$.

4. CNN-BILSTM-OC Lime Rotary Kiln Temperature Prediction Model

4.1. Convolutional neural networks (CNN model)

The convolutional neural networks model possesses the feature of weight sharing; its local range of features is consistent with the global. This model can reduce the dimensionality of the data, starting from the local perspective to analyze the global attributes, so this model is widely used to process some complex situations. Its basic structural framework is shown in Fig. 3.

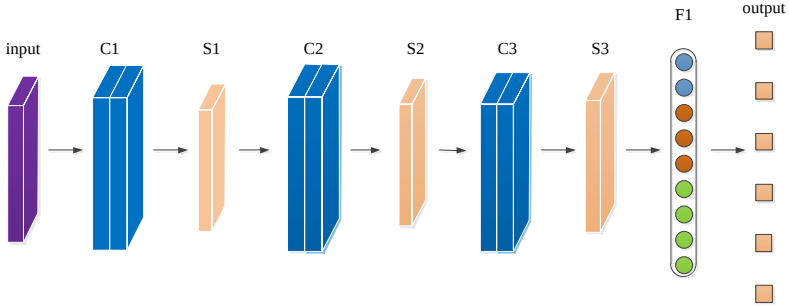

Fig. 3. Convolutional Neural Network structure

The convolutional neural network first analyzes and processes the input data using a sliding convolution kernel window and extracts vector features in the local range through the sliding window, in which the computational process of the convolution kernel to extract the data features is shown in Eq. (10)[15]. After the convolution of the convolution kernel window convolution of the data features need to go through the downsampling layer of the extracted features for screening and analysis, compression of similar feature representations, reduce the complexity of the convolution model, so the convolution and downsampling layers are generally stacked, and the extracted features can repeatedly reduce dimensionality. This model uses the maximum pooling method to reduce the model feature dimensionality; its calculation process is shown in Eq. (11). After the pooling and dimensionality reduction, the features must select different activation functions for activation analysis[16]. This model uses the ReLU activation function, which can significantly improve the convergence speed of the model, and there is no gradient disappearance; the activation form is shown in Eq. (12).

$$y_{l,n}(m) = w_{l-1,n} x_{l-1}(m) + b_{l-1,n} \tag{10}$$

$$r_j = \max_{1<i<l}\left(p_{i,j}\right) \tag{11}$$

$$\mathrm{Re}\,LU = \begin{cases} x & x > 0 \\ 0 & x \le 0 \end{cases} \tag{12}$$

Where $y_{l,n}(m)$ is the convolution output value; $w_{l\text{-}1,n}$ is the weight value; $x_{l\text{-}1}(m)$ is the convolution input value; $b_{l\text{-}1,n}$ is the bias value; r_j is the region maximum; l is the interval length; ReLU is the activation function.

4.2. Bi-directional Long Short-Term Memory Networks (BiLSTM model)

The lime rotary kiln system under the combustion state is a dynamic cycle system that constantly changes, and the parameters measured by the model continue to change in this state. The current and historical moment data strongly influence the model's predictions, so they need to be analyzed and processed in combination with the overall before and after the state of the system[17]. When traditional recurrent neural networks deal with long time series data, there is a possibility that the gradient explosion or disappearance may occur in the memory prediction of the past data. In contrast, Bi-directional Long Short-Term Memory networks not only propagate the information features positively from the starting point but also propagate the information features negatively from the end[18]. Through the associated use of input gate, output gate, forgetting gate, and other memory units, the Bi-directional Long Short-Term Memory network is similar to the human brain, which constantly forgets the non-important features and strengthens the weights of essential features in the model cycle, to achieve better prediction results. Its structural model is shown in Fig. 4.

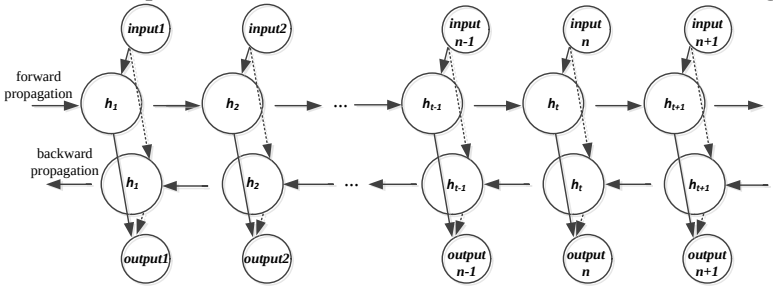

Fig. 4. Bi-directional Long Short-Term Memory networks structure

The prediction model can save the data features at a specific moment through forward and backward propagation, and the specific computational process is shown as follows[19].

$$\overrightarrow{h_t} = f\left(\overrightarrow{w_1}\overrightarrow{x_t} + \overrightarrow{w_2}\overrightarrow{h_{t-1}}\right) \tag{13}$$

$$\overleftarrow{h_t} = f\left(\overleftarrow{w_3}\overleftarrow{x_t} + \overleftarrow{w_4}\overleftarrow{h_{t-1}}\right) \tag{14}$$

$$p_t = g\left(\overrightarrow{w_5}\overrightarrow{h_t} + \overleftarrow{w_6}\overleftarrow{h_t}\right) \tag{15}$$

Where $\overrightarrow{h_t}$ is the forward propagation output value; f, g are different function correspondences; w_i is different weights; $\overrightarrow{x_t}$ is the forward propagation input value; $\overleftarrow{h_t}$ is the backward propagation output value; $\overleftarrow{x_t}$ is the backward propagation input value; p_t is the final value.

4.3. CNN-BILSTM-OC Prediction Modeling

4.3.1 Data dynamic error offset time lag compensation analysis

During the data acquisition process, the lime rotary kiln has been in a dynamic combustion working state, which is a typical significant time lag and multi-coupling model, and some data values may have minor dynamic errors[20]. In order to determine the time lag and inertia order of the combustion system of the lime rotary kiln, the model is analyzed using the method based on the error performance criterion. We establish the time-lag inertia model using the secondary airflow input parameter and the temperature output parameter. It is assumed that the predicted temperature of the lime rotary kiln system at time t can be expressed as:

$$y(t)=\sum_{\tau=1}^{\tau_{\max}}\alpha x(t-\tau)+\sum_{d=1}^{d_{\max}}\beta y(t-d) \tag{16}$$

Where y(t) is the output parameter at t-moment; x(t) is the input parameter at t-moment; τ is the system time lag; d is the system inertia; α and β are the time lag and inertia weighting coefficients.

Different time lag and inertia steps are experimented on analysis for the same set of input parameters. Through the selected degree of fit of the error function to identify the model time lag and inertia order selection is good or bad, this paper selects the mean-square error as the error performance criterion, the specific calculation is shown in Eq. (17).

$$E_{MSE}=\frac{1}{n}\sum_{i=1}^{n}\left(y(t)-y'(t)\right)^{2} \tag{17}$$

Where n is the data number; y(t) is the predicted value; y'(t) is the real value.

In order to verify the time lag and inertia of the system, three control data of different periods under a steady combustion state were re-selected for comparative analysis as shown in Fig. 5.

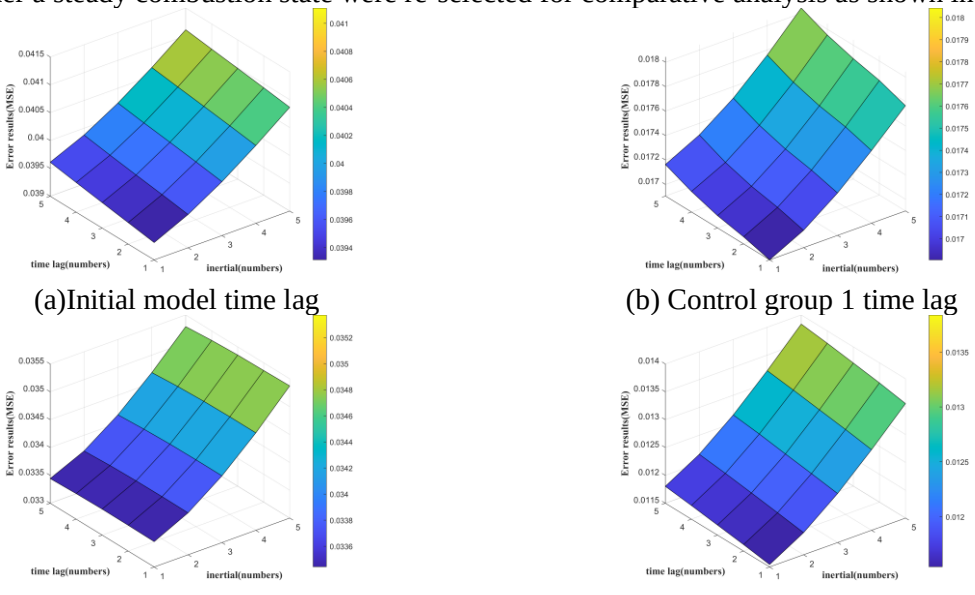

(a)Initial model time lag (b) Control group 1 time lag

(c) Control group 2 time lag (d) Control group 3 time lag

Fig. 5. Analysis of time delay and inertia in lime rotary kiln systems

Analysis of the lime rotary kiln time lag and inertia results show that in the time lag order is less than 2, inertia order is less than 2, the error calculation results of the magnitude of change are less than 0.0005, the overall trend of change is more gentle. When exceeding the node, the surface out of the

face of the inflection point, the calculation error began to climb, indicating that the selected time lag and inertia do not comply with the model of the actual situation, which results in the model overall error gradually become more significant. After analyzing the lime rotary kiln system, time lag and inertia order can be determined as 2, so using the dynamic error offset time lag compensation method to fit the output data to compensate for the analysis; the main calculation steps are shown below:

Step 1: Calculate the offset error amount at the current moment according to Eq. (18) for the predicted output temperature data;

Step 2: Obtain an overall error offset of the output value according to the calculation process shown in Eq. (19);

Step 3: Calculate the error correction value of the output data by substituting the above obtained overall error offset into Eq. (20) to obtain the final result.

$$\delta(t) = y(t-1) - y_s(t-1) \tag{18}$$

$$\delta'(t) = \lambda\delta(t) + (1-\lambda)\delta(t-1) \tag{19}$$

$$y'(t) = y_s(t) + \delta'(t) \tag{20}$$

where δ(t) is the amount of offset error at the current moment; $y(t\text{-}1)$ is the ex-true value; $y_s(t\text{-}1)$ is the ex-predicted value; δ'(t) is the overall error offset; λ is the weight coefficient; $y'(t)$ is the error correction value.

4.3.2 Basic workflow of the prediction model

In order to accurately control the overall state of the lime rotary kiln, this paper proposes a hybrid neural network prediction model based on dynamic error time lag compensation, using the modules in an organic linear overlay. The prediction model mainly comprises a data source pre-processing module, convolutional neural networks module, bi-directional long short-term memory networks module, and error offset dynamic time lag compensation module. The basic flow of the prediction model is shown in Fig. 6.

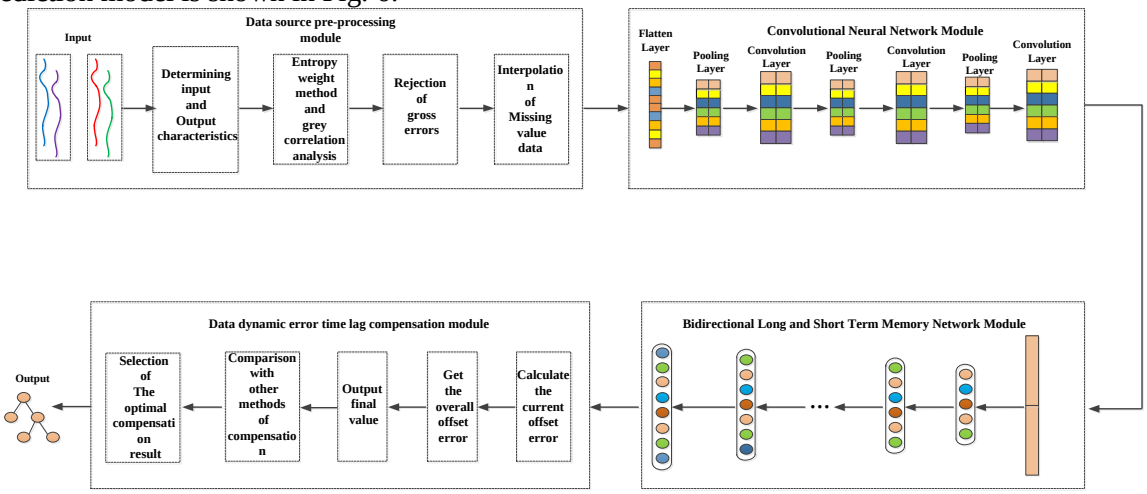

Fig. 6. CNN-BILSTM-OC model flowchart

The basic workflow is as follows: First, analyze the process flow of the lime rotary kiln operation to get the input and output characteristics of the lime rotary kiln prediction model, after the data source pre-processing module for the initial data set entropy and grey correlation analysis and data smoothing, transformed into the form of the input in line with the prediction model, and then pass through the convolutional neural network module and bi-directional long short-term memory network

module for feature extraction processing and time series prediction analysis of the data, and finally for the prediction results obtained by the model for the data dynamic error offset time lag compensation, and the actual data for comparison and analysis, and constantly adjusting the model parameters so that the prediction error is minimized.

5. The Lime rotary kiln prediction model's simulation experiment analysis

5.1. Data set analysis

This experiment takes the lime rotary kiln of the China Shougang Changgang Steel as the research object. The sampling interval is 5 minutes, and 2000 sets of data are selected as the model data set, of which 80% were used as the training set and 20% as the test set. The data set was calculated using Matlab 2019b. The field technicians can measure the flow rate of each parameter the model requires using the Verabar flowmeter (product type: AKLT-BL)(measurement standard: JJG 640-2016) fixed to the port of the input pipe. Wind pressure can be measured by the air pressure sensor(product type: CYYZ16A)(measurement standard: GB/T 42567.2-2023). The kiln temperature can be obtained by fixing a colorimetric thermometer (product type: SA-2S400A)(measurement standard: GB/T 36014.2-2020) on the surface of the kiln shell. The total amount of pulverized coal is calculated from the amount fed by the rotor conveyor (product type: ZTZJ-1200). The pulverized coal feed can be obtained by calculating the times of coal feed from the rotor weigher and the fixed amount of coal feed at each time. Among them, the measurement error and repeatability of the Verabar flowmeter are ±1%, the measurement error of the colorimetric thermometer is ±0.5% of the range, the comprehensive accuracy of the air pressure sensor is 0.5%FS (FS is the maximum range of the air pressure sensor). Errors caused by the measuring instruments do not affect the overall trend of the data and the range of the intervals in which each parameter is located but only cause slight fluctuations in the data. Datasets that have been smoothed and preprocessed do not affect model construction and computation. The sample data set is shown in Tab. 1.

Table 1. Examples of data sets

influencing factors	a (m^3/h)	b (m^3/h)	c (m^3/h)	d (m^3/h)	e (Kpa)	f (Kpa)	g (pa)	h (Hz)	i (t)	g (℃)
1	4445.59	5214.35	3277.95	20776.7	25.8561	3.18461	-3284.51	24.6246	146.081	1340.59
2	4658.27	5194.06	3295.22	21520.9	25.8496	3.182	-3284.14	24.5911	146.301	1340.59
…	…	…	…	…	…	…	…	…	…	…
2000	4883.56	5065.79	4410.02	19701.7	16.8229	2.38571	-3839.34	24.6002	273.241	1348.59

a-coke oven gas flow; b-mixed gas flow; c-the primary air flow; d-the secondary air flow; e-the primary air pressure; f-the secondary air pressure; g-the central induced air pressure; h-kiln spindle frequency; i-the total amount of material fed;g-kiln temperature

5.2. Evaluation indexes

In order to scientifically evaluate the prediction performance of the model, this paper adopts the root mean square error (RMSE) and the mean absolute error (MAE) as the indexes to judge the model's accuracy. The calculation process is shown in Eq. (21) and Eq. (22).

$$RMSE = \sqrt{\frac{1}{n}\sum_{i=1}^{n}\left(x_i - x_i^{'}\right)^2} \tag{21}$$

$$MAE = \frac{1}{n}\sum_{i=1}^{n}\left|x_i - x_i^{'}\right| \tag{22}$$

Where n is the number of data; x_i is the predicted result value; $x_i^{'}$ is the measured true value.

5.3. Comparative analysis of different model prediction results

In order to verify the superiority of the performance of the CNN-BILSTM-OC prediction model proposed in this paper, it is necessary to compare this model with other control group experiments, select traditional neural networks such as CNN, BILSTM, and RF as the model control group. At the same time, compare the actual data model, the compensation model based on the least-squares method, and the compensation model based on the time lag of the dynamic error. Then, analyze the compensation model in different ways. The superiority of the model performance and the comparison of the different model's specific prediction error results are shown in Fig. 7, and the comparison of model numerical errors are shown in Tab. 2.

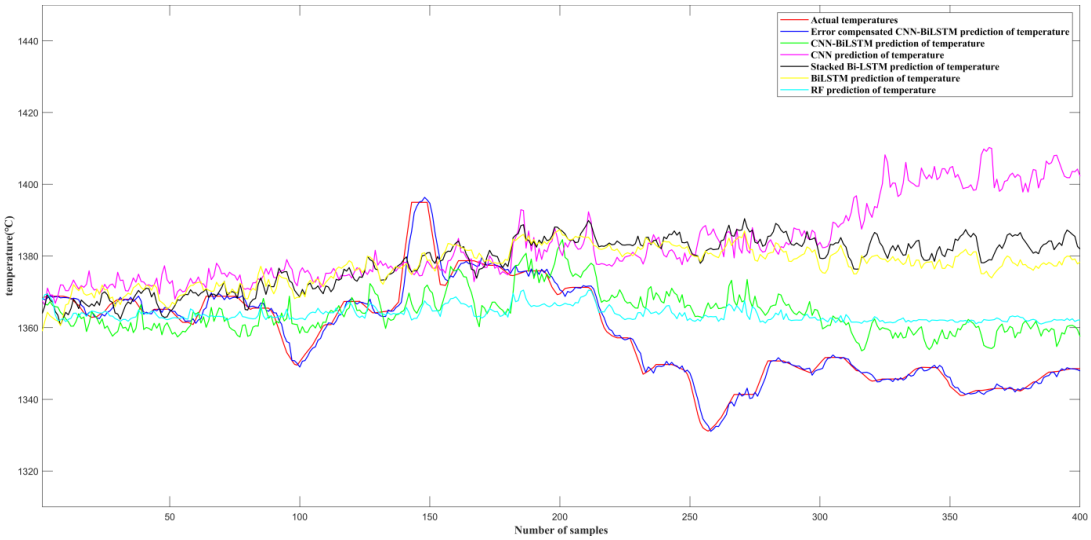

Fig. 7. Comparison of the errors of different models

Table 2. Numerical analysis of prediction errors of different models

Algorithmic Models	root mean square error (RMSE)	mean absolute error (MAE)
CNN	28.9842	22.785
BILSTM	25.6926	21.0024
Stacked BILSTM	24.9644	19.9656
RF	13.3782	10.8473
CNN-BILSTM	10.9289	8.2918
CNN-BILSTM-LSM	1.3027	0.76312
CNN-BILSTM-OC	0.8553	0.61659

The above figures show that all the evaluation indexes of the fusion neural network prediction model based on dynamic error time lag compensation are lower than those of the control model. The

prediction datas obtained from the CNN-BILSTM-OC model have a minor error with the actual temperature data, and the prediction curve is the closest to the actual curve.

After comparing the error data, it can be quantified that the CNN-BILSTM fusion model, compared to the CNN model, reduced the RMSE by 62.29% and the MAE by 63.61%. Compared to the BILSTM model, the RMSE was reduced 57.46%, and the MAE was decreased by 60.52%. Compared to the stacked BILSTM model reduced the RMSE by 56.22% and the MAE by 58.47%. Compared to the RF model reduced the RMSE by 18.31% and the MAE by 23.56%. At the same time, the model's accuracy after compensation is greatly improved compared with that of the uncompensated model. After compensation for dynamic error time lag, the prediction model reduced the RMSE by 34.34% and the MAE by 19.20% compared with the prediction model based on the least squares compensation, making the compensation accuracy more favorable. Based on the quantitative comparison of the relative and absolute prediction errors of the above-proposed model, the overall error situation of the model is analyzed, and the specific distribution is shown in Fig. 8.

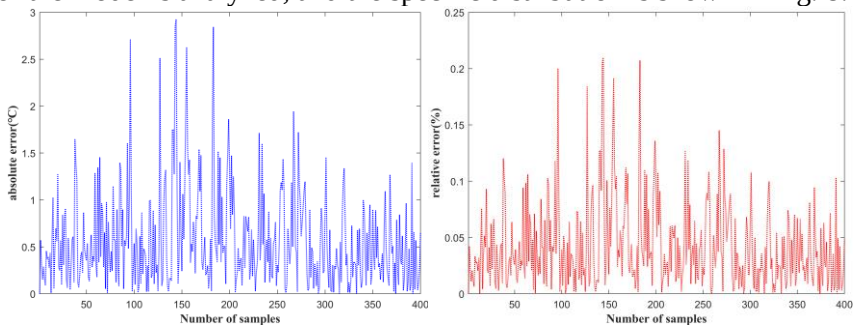

Fig. 8. CNN-BILSTM-OC model of absolute and relative errors

Figure 8 can be analyzed to show that the prediction circumstances of the CNN-BILSTM-OC model can accurately express the system state at the current moment. The maximum absolute error of the prediction results of the CNN-BILSTM-OC model in the dataset of this paper is 2.926℃, and the maximum relative error is 0.2098%, which meets the practical use requirements. Compared with other prediction models, the absolute error in predicted temperature derived from this paper is smaller, with a maximum temperature error temperature of 2.926°C and an average temperature error value of 0.5711°C, which is better than the temperature prediction error value of 3.16°C of other model 1, it also outperforms the predicted temperature of 3.51°C presented in model 2.

Meanwhile, to verify the generalization performance of the CNN-BILSTM-OC model, the three sets of control data used above are selected to compare the generalization ability of this model under different working conditions, and the model prediction results are shown in Fig. 9.

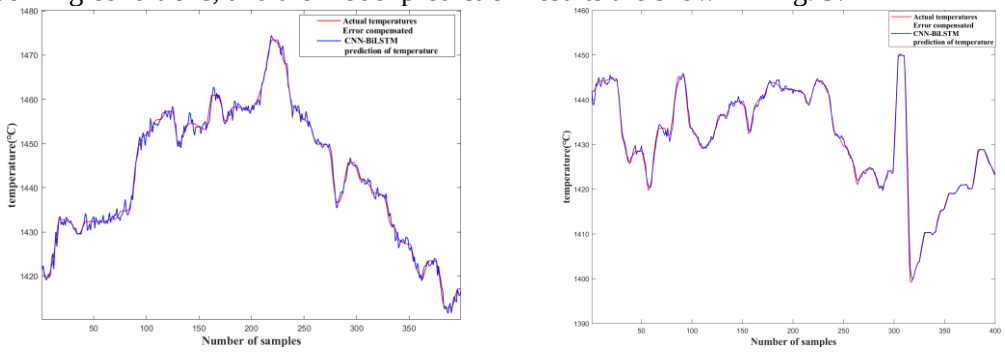

(a) Predicted results for control Group 1 (b) Predicted results for control Group 2

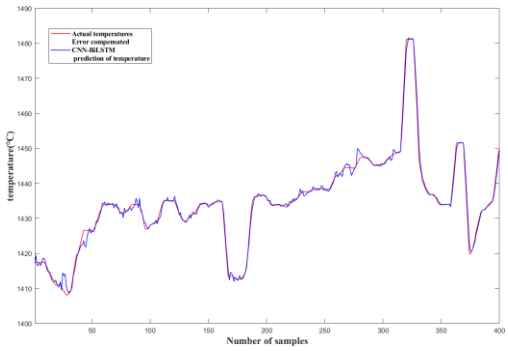

(c) Predicted results for control Group 3

Fig. 9. Prediction results of CNN-BILSTM-OC model under different working conditions

The above figures show that the CNN-BILSTM-OC model can accurately predict the temperature data of the lime rotary kiln combustion system under different operating conditions. The control group 1 RMSE is 1.0487, and the MAE is 0.81019; the control group 2 RMSE is 0.77677, and the MAE is 0.51023; the control group 3 RMSE is 1.0664, and the MAE is 0.68443; it can be calculated that the generalized mean of the root mean square error of the model is 0.9639, and the generalized mean absolute error is 0.6683. Experimentally, it is proved that the prediction performance of the CNN-BILSTM-OC model is more excellent under different working conditions, and the prediction error is small, which can reflect the strong generalization ability of the model.

6. Conclusion

1) This paper proposes a hybrid neural network lime rotary kiln temperature prediction model based on dynamic error time lag compensation. The validity and relevance of the relevant factors of the initial data of the model are analyzed and verified through the entropy and grey correlation degree hybrid algorithm. The initial data set is preprocessed to facilitate the use of the subsequent prediction model.

2) This prediction model can take into account the spatial feature extraction as well as the feature capture of the temporal series, analyze the time lag and inertia order of the lime rotary kiln combustion system and compensate the model, and verify the superiority of the compensation method proposed in this paper by comparing it with the other compensation models. The prediction results of the hybrid neural network model of CNN-BILSTM-OC are higher in accuracy and smaller in prediction error compared to the prediction results of the other models, and the fusion prediction model reduces the error of the prediction results by about 18% compared with optimal other classical models.

3) The model proposed in this paper can compensate for the changes in model prediction accuracy due to data acquisition and system time lag errors. At the same time, it is verified that the CNN-BILSTM-OC model has a better generalization ability under different working conditions, the generalization average of the root mean square error of the temperature prediction data obtained is 0.9639, and that the generalization average of the mean absolute error is 0.6683, which can precisely realize the temperature prediction of lime rotary kiln system.

References

[1] Hu, Y., *et al.*, Working Condition Recognition Based on Transfer Learning and Attention

Mechanism for a rotary kiln, Entropy, *24*(2022), 9, pp. 1186
[2] Urbano, J. J., *et al*., Dynamic modeling of the heat transfer process in rotary kilns with indirect oil heating: Parametric analysis of gypsum calcination case, Thermal Science, *26*(2022), 2 Part C, pp. 1637-1648
[3] Li, J., *et al*., DTDR–ALSTM: Extracting dynamic time-delays to reconstruct multivariate data for improving attention-based LSTM industrial time series prediction models, Knowledge-Based Systems, *211*(2021), pp. 106508
[4] Tian, Z. D., *et al*., SVM predictive control for calcination zone temperature in lime rotary kiln with improved PSO algorithm, Transactions of the Institute of Measurement and Control, *40*(2018), 10, pp. 3134–3146
[5] Zhang, R. F., *et al*., Recognition method of cement rotary kiln burning state based on Otsu-Kmeans flame image segmentation and SVM, Optik, *243*(2021), pp. 167418
[6] Chen, H., *et al*., Recognition of the Temperature Condition of a rotary kiln Using Dynamic Features of a Series of Blurry Flame Images, IEEE transactions on industrial informatics, *12*(2016), 1, pp. 148-157
[7] Hu, W. Y., Mao, Z. Z., Forecasting for Chaotic Time Series Based on GRP-lstmGAN Model: Application to Temperature Series of rotary kiln, Entropy, *25*(2022), 1, pp. 52
[8] Xu, K. K., *et al*., Cement rotary kiln temperature prediction based on time-delay calculation and residual network and bidirectional novel gated recurrent unit multi-model fusion, Measurement, *218*(2023), pp. 113123
[9] Zheng, J. Q., *et al*., Hybrid model of a cement rotary kiln using an improved attention-based recurrent neural network, ISA transactions, *129*(2022), pp. 631-643
[10] Wang, W., *et al*., A soft sensor modeling method with dynamic time-delay estimation and its application in wastewater treatment plant, Biochemical Engineering Journal, *172*(2021), pp. 108048
[11] Okoji, A. I., *et al*., Energetic assessment of a precalcining rotary kiln in a cement plant using process simulator and neural networks, Alexandria Engineering Journal, *61*(2022), 7, pp. 5097-5109
[12] Li, P., *et al*., A synergy model of material and energy flow analysis for the calcination process of green petroleum coke in rotary kiln, Thermal Science, *26*(2022), 2 Part C, pp. 1809-1823
[13] Xue, H. B., *et al*., Data Quality Evaluation of Photovoltaic Power Station based on Entropy Weight Method and Grey Comprehensive Evaluation Method, Journal of Physics: Conference Series, *2399*(2022), 1, pp. 012001
[14] Edmund, W. M., Numerical Calculus, Princeton University Press., Princeton, USA, 2015
[15] Alzahrani, S., *et al*., Continuous Mobile User Authentication Using a Hybrid CNN-Bi-LSTM Approach, CMC-COMPUTERS MATERIALS & CONTINUA, *75*(2023), 1, pp. 651-667
[16] Guo, Y. L., Mao, Z. Z., Long-Term Prediction Model for NOx Emission Based on LSTM–Transformer, Electronics, *12*(2023), 18, pp.3929
[17] Tao, L., *et al*., Rotary kiln Combustion State Recognition Based on Convolutional Neural Network, Journal of Physics:Conference Series, *1575*(2020), 1, pp.012030
[18] Wang, N. E., Li, Z. M., Short term power load forecasting based on BES-VMD and CNN-Bi-LSTM method with error correction, Frontiers in Energy Research, *10*(2023), pp. 1076529
[19] Xiong, W. L., *et al*., JITL based MWGPR soft sensor for multi-mode process with dual-updating

strategy, Computers and Chemical Engineering, *90*(2016), pp. 260-267
[20] Guo, X. F., *et al*., RUL prediction of lithium ion battery based on CEEMDAN-CNN BiLSTM model, Energy Reports, *9*(2023), pp. 1299-1306

Submitted: 02.09.2023.
Revised: 26.10.2023.
Accepted: 02.11.2023.